

Measurement of J/ψ Azimuthal Anisotropy in Au+Au Collisions at $\sqrt{s_{NN}} = 200$ GeV

L. Adamczyk,¹ J. K. Adkins,²³ G. Agakishiev,²¹ M. M. Aggarwal,³⁴ Z. Ahammed,⁵³ I. Alekseev,¹⁹ J. Alford,²² C. D. Anson,³¹ A. Aparin,²¹ D. Arkhipkin,⁴ E. Aschenauer,⁴ G. S. Averichev,²¹ J. Balewski,²⁶ A. Banerjee,⁵³ Z. Barnovska,¹⁴ D. R. Beavis,⁴ R. Bellwied,⁴⁹ M. J. Betancourt,²⁶ R. R. Betts,¹⁰ A. Bhasin,²⁰ A. K. Bhati,³⁴ Bhattacharai,⁴⁸ H. Bichsel,⁵⁵ J. Bielcik,¹³ J. Bielcikova,¹⁴ L. C. Bland,⁴ I. G. Bordyuzhin,¹⁹ W. Borowski,⁴⁵ J. Bouchet,²² A. V. Brandin,²⁹ S. G. Brovko,⁶ E. Bruna,⁵⁷ S. Bültmann,³² I. Bunzarov,²¹ T. P. Burton,⁴ J. Butterworth,⁴⁰ X. Z. Cai,⁴⁴ H. Caines,⁵⁷ M. Calderón de la Barca Sánchez,⁶ D. Cebra,⁶ R. Cendejas,³⁵ M. C. Cervantes,⁴⁷ P. Chaloupka,¹³ Z. Chang,⁴⁷ S. Chattopadhyay,⁵³ H. F. Chen,⁴² J. H. Chen,⁴⁴ J. Y. Chen,⁹ L. Chen,⁹ J. Cheng,⁵⁰ M. Cherney,¹² A. Chikanian,⁵⁷ W. Christie,⁴ P. Chung,¹⁴ J. Chwastowski,¹¹ M. J. M. Codrington,⁴⁸ R. Corliss,²⁶ J. G. Cramer,⁵⁵ H. J. Crawford,⁵ X. Cui,⁴² S. Das,¹⁶ A. Davila Leyva,⁴⁸ L. C. De Silva,⁴⁹ R. R. Debbé,⁴ T. G. Dedovich,²¹ J. Deng,⁴³ R. Derradi de Souza,⁸ S. Dhamija,¹⁸ B. di Ruzza,⁴ L. Didenko,⁴ F. Ding,⁶ A. Dion,⁴ P. Djawotho,⁴⁷ X. Dong,²⁵ J. L. Drachenberg,⁵² J. E. Draper,⁶ C. M. Du,²⁴ L. E. Dunkelberger,⁷ J. C. Dunlop,⁴ L. G. Efimov,²¹ M. Elnimr,⁵⁶ J. Engelage,⁵ G. Eppley,⁴⁰ L. Eun,²⁵ O. Evdokimov,¹⁰ R. Fatemi,²³ S. Fazio,⁴ J. Fedorisin,²¹ R. G. Fersch,²³ P. Filip,²¹ E. Finch,⁵⁷ Y. Fisysak,⁴ E. Flores,⁶ C. A. Gagliardi,⁴⁷ D. R. Gangadharan,³¹ D. Garand,³⁷ F. Geurts,⁴⁰ A. Gibson,⁵² S. Gliske,² O. G. Grebenyuk,²⁵ D. Grosnick,⁵² A. Gupta,²⁰ S. Gupta,²⁰ W. Guryn,⁴ B. Haag,⁶ O. Hajkova,¹³ A. Hamed,⁴⁷ L.-X. Han,⁴⁴ J. W. Harris,⁵⁷ J. P. Hays-Wehle,²⁶ S. Heppelmann,³⁵ A. Hirsch,³⁷ G. W. Hoffmann,⁴⁸ D. J. Hofman,¹⁰ S. Horvat,⁵⁷ B. Huang,⁴ H. Z. Huang,⁷ P. Huck,⁹ T. J. Humanic,³¹ G. Igo,⁷ W. W. Jacobs,¹⁸ C. Jena,³⁰ E. G. Judd,⁵ S. Kabana,⁴⁵ K. Kang,⁵⁰ J. Kapitan,¹⁴ K. Kauder,¹⁰ H. W. Ke,⁹ D. Keane,²² A. Kechechyan,²¹ A. Kesich,⁶ D. P. Kikola,³⁷ J. Kiryluk,²⁵ I. Kisel,²⁵ A. Kisiel,⁵⁴ S. R. Klein,²⁵ D. D. Koetke,⁵² T. Kollegger,¹⁵ J. Konzer,³⁷ I. Koralt,³² W. Korsch,²³ L. Kotchenda,²⁹ P. Kravtsov,²⁹ K. Krueger,² I. Kulakov,²⁵ L. Kumar,²² M. A. C. Lamont,⁴ J. M. Landgraf,⁴ K. D. Landry,⁷ S. LaPointe,⁵⁶ J. Lauret,⁴ A. Lebedev,⁴ R. Lednicky,²¹ J. H. Lee,⁴ W. Leight,²⁶ M. J. LeVine,⁴ C. Li,⁴² W. Li,⁴⁴ X. Li,³⁷ X. Li,⁴⁶ Y. Li,⁵⁰ Z. M. Li,⁹ L. M. Lima,⁴¹ M. A. Lisa,³¹ F. Liu,⁹ T. Ljubicic,⁴ W. J. Llope,⁴⁰ R. S. Longacre,⁴ Y. Lu,⁴² X. Luo,⁹ A. Luszczak,¹¹ G. L. Ma,⁴⁴ Y. G. Ma,⁴⁴ D. M. M. D. Madagadgettige Don,¹² D. P. Mahapatra,¹⁶ R. Majka,⁵⁷ S. Margetis,²² C. Markert,⁴⁸ H. Masui,²⁵ H. S. Matis,²⁵ D. McDonald,⁴⁰ T. S. McShane,¹² S. Mioduszewski,⁴⁷ M. K. Mitrovski,⁴ Y. Mohammed,⁴⁷ B. Mohanty,³⁰ M. M. Mondal,⁴⁷ M. G. Munhoz,⁴¹ M. K. Mustafa,³⁷ M. Naglis,²⁵ B. K. Nandi,¹⁷ Md. Nasim,⁵³ T. K. Nayak,⁵³ J. M. Nelson,³ L. V. Nogach,³⁶ J. Novak,²⁸ G. Odyniec,²⁵ A. Ogawa,⁴ K. Oh,³⁸ A. Ohlson,⁵⁷ V. Okorokov,²⁹ E. W. Oldag,⁴⁸ R. A. N. Oliveira,⁴¹ D. Olson,²⁵ M. Pachr,¹³ B. S. Page,¹⁸ S. K. Pal,⁵³ Y. X. Pan,⁷ Y. Pandit,¹⁰ Y. Panebratsev,²¹ T. Pawlak,⁵⁴ B. Pawlik,³³ H. Pei,¹⁰ C. Perkins,⁵ W. Peryt,⁵⁴ P. Pile,⁴ M. Planinic,⁵⁸ J. Pluta,⁵⁴ N. Poljak,⁵⁸ J. Porter,²⁵ A. M. Poskanzer,²⁵ C. B. Powell,²⁵ C. Pruneau,⁵⁶ N. K. Pruthi,³⁴ M. Przybycien,¹ P. R. Pujahari,¹⁷ J. Putschke,⁵⁶ H. Qiu,²⁵ S. Ramachandran,²³ R. Raniwala,³⁹ S. Raniwala,³⁹ R. L. Ray,⁴⁸ C. K. Riley,⁵⁷ H. G. Ritter,²⁵ J. B. Roberts,⁴⁰ O. V. Rogachevskiy,²¹ J. L. Romero,⁶ J. F. Ross,¹² L. Ruan,⁴ J. Rusnak,¹⁴ N. R. Sahoo,⁵³ P. K. Sahu,¹⁶ I. Sakrejda,²⁵ S. Salur,²⁵ A. Sandacz,⁵⁴ J. Sandweiss,⁵⁷ E. Sangaline,⁶ A. Sarkar,¹⁷ J. Schambach,⁴⁸ R. P. Scharenberg,³⁷ A. M. Schmah,²⁵ B. Schmidke,⁴ N. Schmitz,²⁷ T. R. Schuster,¹⁵ J. Seger,¹² P. Seyboth,²⁷ N. Shah,⁷ E. Shalahiev,²¹ M. Shao,⁴² B. Sharma,³⁴ M. Sharma,⁵⁶ S. S. Shi,⁹ Q. Y. Shou,⁴⁴ E. P. Sichtermann,²⁵ R. N. Singaraju,⁵³ M. J. Skoby,¹⁸ D. Smirnov,⁴ N. Smirnov,⁵⁷ D. Solanki,³⁹ P. Sorensen,⁴ U. G. deSouza,⁴¹ H. M. Spinka,² B. Srivastava,³⁷ T. D. S. Stanislaus,⁵² J. R. Stevens,²⁶ R. Stock,¹⁵ M. Strikhanov,²⁹ B. Stringfellow,³⁷ A. A. P. Suaide,⁴¹ M. C. Suarez,¹⁰ M. Sumera,¹⁴ X. M. Sun,²⁵ Y. Sun,⁴² Z. Sun,²⁴ B. Surrow,⁴⁶ D. N. Svirida,¹⁹ T. J. M. Symons,²⁵ A. Szanto de Toledo,⁴¹ J. Takahashi,⁸ A. H. Tang,⁴ Z. Tang,⁴² L. H. Tarini,⁵⁶ T. Tarnowsky,²⁸ J. H. Thomas,²⁵ J. Tian,⁴⁴ A. R. Timmins,⁴⁹ D. Tlusty,¹⁴ M. Tokarev,²¹ S. Trentalange,⁷ R. E. Tribble,⁴⁷ P. Tribedy,⁵³ B. A. Trzeciak,⁵⁴ O. D. Tsai,⁷ J. Turnau,³³ T. Ullrich,⁴ D. G. Underwood,² G. Van Buren,⁴ G. van Nieuwenhuizen,²⁶ J. A. Vanfossen, Jr.,²² R. Varma,¹⁷ G. M. S. Vasconcelos,⁸ F. Videbæk,⁴ Y. P. Viyogi,⁵³ S. Vokal,²¹ S. A. Voloshin,⁵⁶ A. Vossen,¹⁸ M. Wada,⁴⁸ F. Wang,³⁷ G. Wang,⁷ H. Wang,⁴ J. S. Wang,²⁴ Q. Wang,³⁷ X. L. Wang,⁴² Y. Wang,⁵⁰ G. Webb,²³ J. C. Webb,⁴ G. D. Westfall,²⁸ C. Whitten Jr.,⁷ H. Wieman,²⁵ S. W. Wissink,¹⁸ R. Witt,⁵¹ Y. F. Wu,⁹ Z. Xiao,⁵⁰ W. Xie,³⁷ K. Xin,⁴⁰ H. Xu,²⁴ N. Xu,²⁵ Q. H. Xu,⁴³ W. Xu,⁷ Y. Xu,⁴² Z. Xu,⁴ L. Xue,⁴⁴ Y. Yang,²⁴ Y. Yang,⁹ P. Yepes,⁴⁰ L. Yi,³⁷ K. Yip,⁴ I.-K. Yoo,³⁸ M. Zawisza,⁵⁴ H. Zbroszczyk,⁵⁴ J. B. Zhang,⁹ S. Zhang,⁴⁴ X. P. Zhang,⁵⁰ Y. Zhang,⁴² Z. P. Zhang,⁴² F. Zhao,⁷ J. Zhao,⁴⁴ C. Zhong,⁴⁴ X. Zhu,⁵⁰ Y. H. Zhu,⁴⁴ Y. Zoukarneeva,²¹ and M. Zyzak²⁵

(STAR Collaboration)

- ¹AGH University of Science and Technology, Cracow, Poland
- ²Argonne National Laboratory, Argonne, Illinois 60439, USA
- ³University of Birmingham, Birmingham, United Kingdom
- ⁴Brookhaven National Laboratory, Upton, New York 11973, USA
- ⁵University of California, Berkeley, California 94720, USA
- ⁶University of California, Davis, California 95616, USA
- ⁷University of California, Los Angeles, California 90095, USA
- ⁸Universidade Estadual de Campinas, Sao Paulo, Brazil
- ⁹Central China Normal University (HZNU), Wuhan 430079, China
- ¹⁰University of Illinois at Chicago, Chicago, Illinois 60607, USA
- ¹¹Cracow University of Technology, Cracow, Poland
- ¹²Creighton University, Omaha, Nebraska 68178, USA
- ¹³Czech Technical University in Prague, FNSPE, Prague, 115 19, Czech Republic
- ¹⁴Nuclear Physics Institute AS CR, 250 68 Řež/Prague, Czech Republic
- ¹⁵University of Frankfurt, Frankfurt, Germany
- ¹⁶Institute of Physics, Bhubaneswar 751005, India
- ¹⁷Indian Institute of Technology, Mumbai, India
- ¹⁸Indiana University, Bloomington, Indiana 47408, USA
- ¹⁹Alikhanov Institute for Theoretical and Experimental Physics, Moscow, Russia
- ²⁰University of Jammu, Jammu 180001, India
- ²¹Joint Institute for Nuclear Research, Dubna, 141 980, Russia
- ²²Kent State University, Kent, Ohio 44242, USA
- ²³University of Kentucky, Lexington, Kentucky, 40506-0055, USA
- ²⁴Institute of Modern Physics, Lanzhou, China
- ²⁵Lawrence Berkeley National Laboratory, Berkeley, California 94720, USA
- ²⁶Massachusetts Institute of Technology, Cambridge, MA 02139-4307, USA
- ²⁷Max-Planck-Institut für Physik, Munich, Germany
- ²⁸Michigan State University, East Lansing, Michigan 48824, USA
- ²⁹Moscow Engineering Physics Institute, Moscow Russia
- ³⁰National Institute of Science and Education and Research, Bhubaneswar 751005, India
- ³¹Ohio State University, Columbus, Ohio 43210, USA
- ³²Old Dominion University, Norfolk, VA, 23529, USA
- ³³Institute of Nuclear Physics PAN, Cracow, Poland
- ³⁴Panjab University, Chandigarh 160014, India
- ³⁵Pennsylvania State University, University Park, Pennsylvania 16802, USA
- ³⁶Institute of High Energy Physics, Protvino, Russia
- ³⁷Purdue University, West Lafayette, Indiana 47907, USA
- ³⁸Pusan National University, Pusan, Republic of Korea
- ³⁹University of Rajasthan, Jaipur 302004, India
- ⁴⁰Rice University, Houston, Texas 77251, USA
- ⁴¹Universidade de Sao Paulo, Sao Paulo, Brazil
- ⁴²University of Science & Technology of China, Hefei 230026, China
- ⁴³Shandong University, Jinan, Shandong 250100, China
- ⁴⁴Shanghai Institute of Applied Physics, Shanghai 201800, China
- ⁴⁵SUBATECH, Nantes, France
- ⁴⁶Temple University, Philadelphia, Pennsylvania, 19122
- ⁴⁷Texas A&M University, College Station, Texas 77843, USA
- ⁴⁸University of Texas, Austin, Texas 78712, USA
- ⁴⁹University of Houston, Houston, TX, 77204, USA
- ⁵⁰Tsinghua University, Beijing 100084, China
- ⁵¹United States Naval Academy, Annapolis, MD 21402, USA
- ⁵²Valparaiso University, Valparaiso, Indiana 46383, USA
- ⁵³Variable Energy Cyclotron Centre, Kolkata 700064, India
- ⁵⁴Warsaw University of Technology, Warsaw, Poland
- ⁵⁵University of Washington, Seattle, Washington 98195, USA
- ⁵⁶Wayne State University, Detroit, Michigan 48201, USA
- ⁵⁷Yale University, New Haven, Connecticut 06520, USA
- ⁵⁸University of Zagreb, Zagreb, HR-10002, Croatia

(Dated: September 20, 2018)

The measurement of J/ψ azimuthal anisotropy is presented as a function of transverse momentum for different centralities in Au+Au collisions at $\sqrt{s_{NN}} = 200$ GeV. The measured J/ψ elliptic flow is consistent with zero within errors for transverse momentum between 2 and 10 GeV/c. Our

measurement suggests that J/ψ with relatively large transverse momentum are not dominantly produced by coalescence from thermalized charm quarks, when comparing to model calculations.

PACS numbers: 25.75.Cj, 12.38.Mh, 14.40.Pq

Quantum chromodynamics (QCD) predicts a quark-gluon plasma (QGP) phase at extremely high temperature and/or density, consisting of deconfined quarks and gluons. Over the past twenty years, heavy quarkonia production in hot and dense nuclear matter has been a topic attracting growing interest. In relativistic heavy-ion collisions the $c\bar{c}$ bound state is subject to dissociation due to the color screening and the change of binding potential in the deconfined medium. As a consequence, the production of J/ψ is expected to be suppressed, and such suppression has been proposed as a signature of QGP formation [1]. However, the J/ψ suppression observed in experiments [2–6] can also be affected by additional cold [7, 8] and hot [9–14] nuclear effects. In particular the recombination of J/ψ from a thermalized charm quark and its antiquark has not been unambiguously established experimentally [11–14]. By measuring J/ψ azimuthal anisotropy, especially its second Fourier coefficient v_2 (elliptic flow), one may disentangle J/ψ from direct pQCD processes and from recombination. J/ψ produced from direct pQCD processes, which do not have initial collective motion, should have little azimuthal preference. In non-central collisions, the produced J/ψ will then gain limited azimuthal anisotropy from azimuthally different absorption due to the different path lengths in azimuth. On the other hand, J/ψ produced from recombination of thermalized charm quarks will inherit the flow of charm quarks, exhibiting considerable flow.

Many models that describe the experimental results of heavy-ion collisions depend on the assumption that light flavor quarks in the medium reach thermalization on a short timescale (~ 0.5 fm/c) [15, 16]. However, the dynamics through which the rapid thermalization happens, are not very clear, and it has not been established to what extent thermalization applies. The flow pattern of heavy quarks provides a unique tool to test the thermalization. With much larger mass than that of light quarks, heavy quarks are more resistant to having their velocity changed, and are thus expected to thermalize much more slowly than light partons. If charm quarks are observed to have sizable collective motion, then light partons, which dominate the medium, should be fully thermalized. The charm quark flow can be measured through open [17] and closed charm particles. The J/ψ is the most prominent for experiment among the latter. However, because the J/ψ production mechanism is not well understood, there is significant uncertainty associated with this probe, since only J/ψ from recombination of charm quarks inherit their flow. A detailed comparison between experimental measurements and models on J/ψ v_2 vs. transverse momentum (p_T) and centrality, in

addition to nuclear modification factor, will shed light on the J/ψ production mechanism and charm quark flow.

This analysis benefits from a large amount of data taken during the RHIC [18] $\sqrt{s_{NN}} = 200$ GeV Au+Au run in the year 2010 by the new data acquisition system of STAR [19], capable of an event rate up to 1 kHz. In addition, the newly installed Time Of Flight (TOF) detector [20] allows STAR to improve electron identification, and background electrons from photon conversion are reduced by one order of magnitude due to less material around the center of the detector setup.

The data presented consist of 360 million minimum bias (MB) events triggered by the coincidence of two Vertex Position Detectors [21], 270 million central events triggered by a large hit multiplicity in the TOF detector [20], and a set of high tower events triggered by signals in the towers of Barrel Electromagnetic Calorimeter (BEMC) [22] exceeding certain thresholds (2.6, 3.5, 4.2, and 5.9 GeV). The high tower sample is equivalent to approximately 7 billion MB events for J/ψ production in the high- p_T region. In addition, in order to cope with the large data volume coming from collisions at high luminosity, a High Level Trigger (HLT) was implemented to reconstruct charged tracks online, select events with J/ψ candidates and tag them for fast analysis. There are 16 million J/ψ enriched events selected by the HLT.

The J/ψ were reconstructed through the $J/\psi \rightarrow e^+e^-$ channel, with a branching ratio of 5.9 %. The daughter tracks of the J/ψ were required to have more than 20 hits in the Time Projection Chamber (TPC) [23], and a distance of closest approach less than 1 cm from the primary vertex. Low momentum electrons and positrons can be separated from hadrons by selecting on the inverse velocity ($0.97 < 1/\beta < 1.03$), which is calculated from the time-of-flight measured by the TOF detector [20] and the path length measured by the TPC. At large momentum ($p > 1.5$ GeV/c), with the energy measured by towers from the BEMC [22], a cut of the momentum to energy ratio ($0.3 < p/E < 1.5$) was applied to select electrons and positrons. The electrons and positrons were then identified by their specific energy loss per unit track length ($\langle dE/dx \rangle$) inside the TPC. More than 15 TPC hits were required to calculate $\langle dE/dx \rangle$. The $\langle dE/dx \rangle$ cut is asymmetric around the expected value for electron, because the lower side is where the hadron $\langle dE/dx \rangle$ lies. It also varies according to whether the candidate track passes the $1/\beta$ and/or p/E cut to optimize efficiency and purity. The combination of cuts on $1/\beta$, p/E and $\langle dE/dx \rangle$ enables electron/positron identification in a wide momentum range. Our measured J/ψ particles cover the rapidity range $-1 < y < 1$, favoring J/ψ near

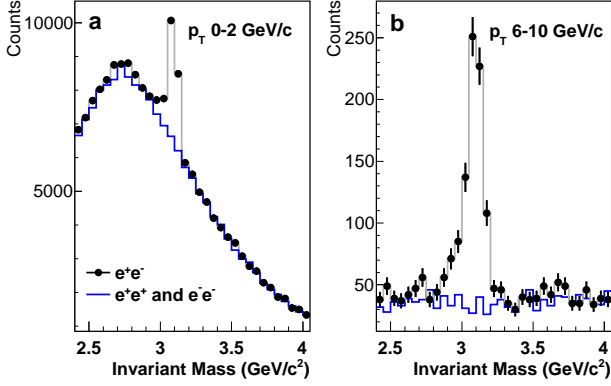


FIG. 1. (color online) Invariant mass spectrum of electron/positron pairs for $0 < p_T < 2$ GeV/c (a) and $6 < p_T < 10$ GeV/c (b). The points are unlike-sign pairs with the J/ψ signal. The blue solid line histogram shows the like-sign background.

$y = 0$ because of detection efficiency variation due to acceptance and decay kinematics.

A total of just over 13000 J/ψ were reconstructed in the entire p_T range of 0-10 GeV/c, and the invariant mass spectra of e^+e^- pairs with the J/ψ signals for the lowest (0-2 GeV/c) and highest (6-10 GeV/c) p_T bins are shown in Fig. 1.

The following method has been used to calculate the v_2 of J/ψ . Firstly, measurements of $\phi - \Psi$, ranging from 0 to π , were divided into 10 bins. Here ϕ is the azimuthal angle of J/ψ , and Ψ is the azimuthal angle of the event plane reconstructed from TPC tracks with the azimuthally nonuniform detector efficiency corrected [24]. Then two bins at supplementary angles were combined into one. The J/ψ yield within a combined $\phi - \Psi$ bin was obtained by fitting the e^+e^- pair invariant mass distribution with a Gaussian signal on top of a second order polynomial background. Then v_2 was obtained by fitting the J/ψ yield vs. $\phi - \Psi$ with a functional form of $A(1 + 2v_2 \cos(2(\phi - \Psi)))$. Finally, the observed v_2 was corrected for the event plane resolution [24].

Three dominant sources of systematic error have been investigated for this measurement: assumptions in the v_2 calculation method, hadron contamination for the daughter e^+e^- pairs, and the non-flow effect. The first source can be estimated from the difference in v_2 calculated by methods with different assumptions. Two other methods are used here. One is similar to the original method except that the J/ψ yield in each combined $\phi - \Psi$ bin was not obtained from fitting, but from subtracting the like-sign background from unlike-sign distribution within the possible invariant mass range of J/ψ . In the other method, the overall v_2 of both signal and background was measured first as a function of invariant mass, and then it was fitted with an average of J/ψ v_2 and back-

ground v_2 weighted by their respective yields vs. invariant mass [25]. The systematic error from hadron contamination can be estimated from the difference in calculated v_2 with different electron/positron identification cuts. While the original cuts aim for the best J/ψ signal, a purer electron/positron sample can be obtained from a set of tighter cuts. The overall systematic uncertainty for the first two sources was estimated from the maximum difference between the calculated v_2 with the $3 \times 2 = 6$ combinations of v_2 methods and electron/positron identification cut sets mentioned above. Besides elliptic flow, there are also some other two- and many-particle correlations due to, for example, resonance decay and jet production. These non-flow correlations may influence the reconstructed event plane and the measured v_2 . To estimate this non-flow influence on the v_2 measurement, a method of scaling non-flow in $p + p$ collisions to that in Au + Au collisions [26] was employed. This method assumes that 1) J/ψ -hadron correlation in $p + p$ collisions is entirely due to non-flow, and 2) the non-flow correlation to other particles per J/ψ in Au + Au collisions is similar to that in $p + p$ collisions. Under these assumptions, it can be deduced that the non-flow influence on measured J/ψ v_2 in Au+Au collisions is $\langle \sum_i \cos 2(\phi_{J/\psi} - \phi_i) \rangle / M \overline{v_2}$. Here the sum is over hadrons and the average is over J/ψ in $p + p$ collisions. M and $\overline{v_2}$ are the multiplicity and average elliptic flow of hadrons in Au+Au collisions, respectively. Since the away side correlation may be greatly modified by the medium in heavy-ion collisions, this procedure gives an upper limit of the non-flow effect. Detector acceptance and efficiency variation with p_T , centrality and rapidity may lead to a biased J/ψ sample, which may induce some systematic effects when v_2 also changes with these parameters. But these effects are estimated to be negligible compared to statistical errors.

Figure 2 shows J/ψ v_2 as a function of transverse momentum for different centralities, with the estimation of non-flow shown by the lines. Data from the central trigger, minimum bias trigger and high tower triggers are used for the 0-10 % most central bin, while only minimum bias and high tower triggered events are used for other centrality bins. Considering errors and the magnitude of non-flow, J/ψ v_2 is consistent with 0 for $p_T > 2$ GeV/c for all measured centrality bins. Light particles usually have a larger v_2 in the intermediate centrality than in the most central and peripheral collisions. This can be explained by a larger initial spatial eccentricity in the intermediate centrality, which is transferred into final state momentum anisotropy due to different pressure gradients in different directions, when there are sufficient interactions in the medium. However, no strong centrality dependence for J/ψ v_2 has been observed in our measurement.

The top panel of Fig. 3 shows J/ψ v_2 for 0 - 80 %

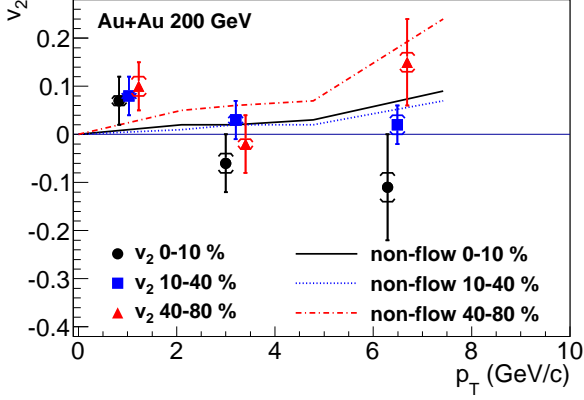


FIG. 2. (color online) v_2 vs. p_T for J/ψ in different centrality bins. The brackets represent systematic errors estimated from differences between different methods and cuts. The p_T bins for J/ψ are 0-2, 2-5 and 5-10 GeV/c. The mean p_T in each bin for the J/ψ sample used for v_2 calculation is drawn, but is shifted a little for some centralities so that all points can be seen clearly. The curves show estimated non-flow influence on measured v_2 (see text).

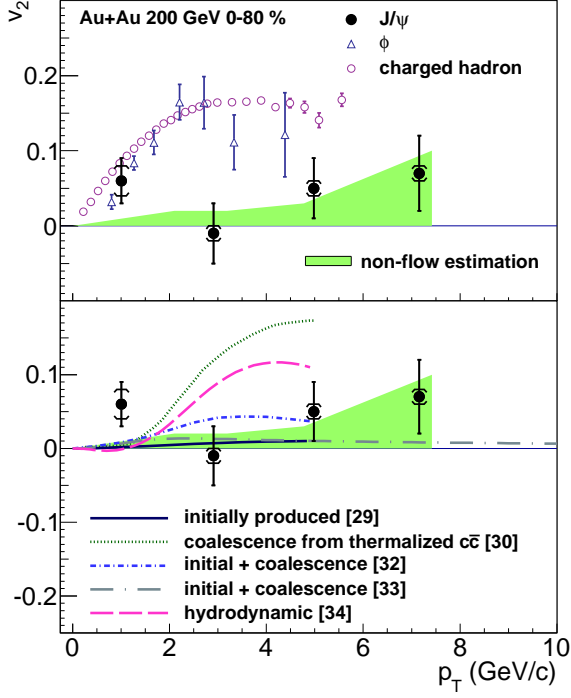


FIG. 3. (color online) v_2 vs. p_T for J/ψ in 0-80 % central events comparing with charged hadrons [27] and the ϕ meson [28] (upper panel) and theoretical calculations [29–34] (lower panel). The brackets represent systematic errors estimated from differences between different methods and cuts. The p_T bins for J/ψ are 0-2, 2-4, 4-6 and 6-10 GeV/c, and the mean p_T in each bin for the J/ψ sample used for v_2 calculation is drawn. Estimated non-flow influence on measured v_2 is shown as the shaded band.

central collisions as a function of transverse momentum. For reference, two other sets of v_2 measurements are also plotted, one is for charged hadrons (dominated by pions) [27] and the other is for the ϕ meson [28] which is heavier than the pion but not as heavy as the J/ψ . Unlike v_2 of hadrons consisting of light quarks, J/ψ v_2 at $p_T > 2$ GeV/c is found to be consistent with zero within statistical errors. However, the significant mass difference between J/ψ and light particles makes the direct comparison of v_2 vs. p_T less conclusive. For example, for the same velocity at $y = 0$, the p_T of J/ψ at 3.0 GeV/c corresponds to p_T of pions (ϕ) at 0.14 (1.0) GeV/c.

In the bottom panel of Fig. 3, a comparison is made between the measured J/ψ v_2 and various theoretical calculations, and a quantitative level of difference is shown in Table I by χ^2/NDF and the p-value. v_2 of J/ψ produced by initial pQCD processes is predicted to stay close to zero [29]. Although both normal suppression due to nuclear absorption and anomalous suppression in the hot medium due to color screening are considered in the model, the azimuthally different suppression along the different path lengths in azimuth leads to a limited v_2 beyond the sensitivity of the current measurement. On the contrary, if charm quarks get fully thermalized and J/ψ are produced by coalescence from the thermalized flowing charm quarks at the freeze-out, the v_2 of J/ψ is predicted to reach almost the same maximum magnitude as v_2 of light flavor mesons, although at a larger p_T (around 4 GeV/c) due to the significantly larger mass of J/ψ [30]. This is 3σ above the measurement for $p_T > 2$ GeV/c, leading to a large χ^2/NDF of 21.1/3 and a small p-value of 1.0×10^{-4} , and is thus inconsistent with the data. Models that include J/ψ from both initial production and coalescence production in the transport model [29, 31] predict a much smaller v_2 [32, 33], and are consistent with our measurement. In these models, J/ψ are formed continuously through the system evolution rather than at the freeze-out, so many J/ψ could be formed from charm quarks whose v_2 has still not fully developed. Furthermore, the initial production of J/ψ with very limited v_2 dominates at high p_T , thus the overall J/ψ v_2 does not rise rapidly as for light hadrons. This kind of model also describes the measured J/ψ nuclear modification factor over a wide range of p_T and centrality [5]. The hydrody-

TABLE I. Difference between model calculations and data. The p-value is the probability of observing a χ^2 that exceeds the current measured χ^2 by chance, even for a correct model.

theoretical calculation	χ^2/NDF	p-value
initially produced [29]	3.7 / 3	2.9×10^{-1}
coalescence from thermalized $c\bar{c}$ [30]	21.1 / 3	1.0×10^{-4}
initial + coalescence [32]	3.7 / 3	3.0×10^{-1}
initial + coalescence [33]	4.9 / 4	3.0×10^{-1}
hydrodynamic [34]	10.1 / 3	1.7×10^{-2}

namic model, which assumes local thermal equilibrium, can be tuned to describe v_2 for light hadrons, but it predicts a J/ψ v_2 that rises strongly with p_T in the region $p_T < 4$ GeV/c, and thus fails to describe the main feature of the data [34]. For heavy particles such as J/ψ , hydrodynamic predictions suffer from large uncertainties related to viscous corrections (δf) at freeze-out and the assumed freeze-out time or temperature.

In summary, J/ψ elliptic flow is presented as a function of transverse momentum for different centralities in $\sqrt{s_{NN}} = 200$ GeV Au+Au collisions. Unlike light flavor hadrons, J/ψ v_2 at $p_T > 2$ GeV/c is consistent with zero within statistical errors. Comparing to model calculations, the measured J/ψ v_2 values disfavor the scenario that J/ψ with $p_T > 2$ GeV/c are produced dominantly by coalescence from (anti-)charm quarks which are thermalized and flow with the medium.

We thank the RHIC Operations Group and RCF at BNL, the NERSC Center at LBNL and the Open Science Grid consortium for providing resources and support. This work was supported in part by the Offices of NP and HEP within the U.S. DOE Office of Science, the U.S. NSF, the Sloan Foundation, CNRS/IN2P3, FAPESP CNPq of Brazil, Ministry of Ed. and Sci. of the Russian Federation, NNSFC, CAS, MoST, and MoE of China, GA and MSMT of the Czech Republic, FOM and NWO of the Netherlands, DAE, DST, and CSIR of India, Polish Ministry of Sci. and Higher Ed., National Research Foundation (NRF-2012004024), Ministry of Sci., Ed. and Sports of the Rep. of Croatia, and RosAtom of Russia.

-
- [1] T. Matsui and H. Satz, Phys. Lett. B **178**, 416 (1986).
 - [2] M. C. Abreu *et al.*, Phys. Lett. B **499**, 85 (2001).
 - [3] A. Adare *et al.*, Phys. Rev. Lett. **98**, 232301 (2007).
 - [4] A. Adare *et al.*, Phys. Rev. C **77**, 024912 (2008).
 - [5] L. Adamczyk *et al.*, e-print arXiv:1208.2736 (2012).

- [6] B. Abelev *et al.*, Phys. Rev. Lett. **109**, 072301 (2012).
- [7] M. B. Johnson *et al.*, Phys. Rev. Lett. **86**, 4483 (2001).
- [8] V. Guzey, M. Strikman, and W. Vogelsang, Phys. Lett. B **603**, 173 (2004).
- [9] R. Baier, D. Schiff, and B. G. Zakharov, Ann. Rev. Nucl. Part. Sci. **50**, 37 (2000).
- [10] S. Gavin and R. Vogt, Nucl. Phys. A **610**, 442C (1996).
- [11] R. L. Thews, Eur. Phys. J. C **43**, 97 (2005).
- [12] R. L. Thews and M. L. Mangano, Phys. Rev. C **73**, 014904 (2006).
- [13] A. Andronic, P. Braun-Munzinger, K. Redlich, and J. Stachel, Nucl. Phys. A **789**, 334 (2007).
- [14] A. Capella *et al.*, Eur. Phys. J. C **58**, 437 (2008).
- [15] P. F. Kolb and U. W. Heinz, in *Quark Gluon Plasma*, edited by R. C. Hwa and X. N. Wang (World Scientific, Singapore, 2003) pp. 634–714.
- [16] P. Huovinen and P. V. Ruuskanen, Ann. Rev. Nucl. Part. Sci. **56**, 163 (2006).
- [17] S. S. Adler *et al.*, Phys. Rev. C **72**, 024901 (2005).
- [18] H. Hahn *et al.*, Nucl. Instrum. Meth. A **499**, 245 (2003).
- [19] K. H. Ackermann *et al.*, Nucl. Instrum. Meth. A **499**, 624 (2003).
- [20] B. Bonner *et al.*, Nucl. Instrum. Meth. A **508**, 181 (2003).
- [21] W. J. Llope *et al.*, Nucl. Instrum. Meth. A **522**, 252 (2004).
- [22] M. Beddo *et al.*, Nucl. Instrum. Meth. A **499**, 725 (2003).
- [23] M. Anderson *et al.*, Nucl. Instrum. Meth. A **499**, 659 (2003).
- [24] A. M. Poskanzer and S. A. Voloshin, Phys. Rev. C **58**, 1671 (1998).
- [25] N. Borghini and J. Y. Ollitrault, Phys. Rev. C **70**, 064905 (2004).
- [26] J. Adams *et al.*, Phys. Rev. Lett. **93**, 252301 (2004).
- [27] J. Adams *et al.*, Phys. Rev. Lett. **92**, 062301 (2004).
- [28] B. I. Abelev *et al.*, Phys. Rev. Lett. **99**, 112301 (2007).
- [29] L. Yan, P. Zhuang, and N. Xu, Phys. Rev. Lett. **97**, 232301 (2006).
- [30] V. Greco, C. M. Ko, and R. Rapp, Phys. Lett. B **595**, 202 (2004).
- [31] L. Ravagli and R. Rapp, Phys. Lett. B **655**, 126 (2007).
- [32] X. Zhao and R. Rapp, e-print arXiv:0806.1239 (2008).
- [33] Y. Liu, N. Xu, and P. Zhuang, Nucl. Phys. A **834**, 317c (2010).
- [34] U. W. Heinz and C. Shen, private communication (2011).